Global Research journal of Natural Science and Technology (Grjnst)
Volume: 03 - Issue 4 (2025)
p.ISSN: 2790-7643 e.ISSN: 2790-7651

Preparation of Charcoal by Combining Bio waste of Selected Fruits and Vegetables

Aysha Saleem

Chemistry, UET, Lahore, Pakistan

ayshasaleem193@gmail.com

Abstract

Bio waste produced from food is naturally biodegradable. The main process for recycling bio waste is pyrolysis, which converts it into charcoal. This study used banana and potato peels to prepare charcoal and investigate its adsorption performance in a combined form. Charcoal was prepared by the pyrolysis of sun-dried and oven-dried bio waste at 500 ℃ separately, then sieved through a 140-mesh screen. The prepared charcoal from both bio wastes was combined in different ratios. It was prepared in native form and activated under acidic and alkaline conditions with HCl and NaOH, respectively. Characterization of the native, acid-activated, and base-activated forms was done using XRD, FTIR, SEM, EDX, methylene blue value, iodine value, ash content, and moisture content. EDX showed that the charcoal contained about 6% impurities. It exhibited aromatic C-H bending and aromatic ring structures. The application of charcoal using methylene blue dye showed that the best adsorbent dose was 0.25 g, the contact time was 40 min, and the initial concentration was 214 ppm. The equilibrium data were best described by the Langmuir isotherm model, with an R^2 value of 0.999, indicating that the adsorption process was monolayer. The data collected through characterization and the application of the prepared charcoal from banana and potato bio waste demonstrate its effectiveness and high adsorption capacity.

Keywords: Bio waste, Native Charcoal, Acid activated Charcoal, Base activated Charcoal

Introduction

Food is a major source of energy in the world and essential for the intake of nutrients [{Pradhan, 2020 #133}; {Rico, 2007 #134}]. Various nutrients in the soil contribute to the production of food-based nutrients [{Pokharel, 2020 #135}]. The global population is increasing day by day [{Foong, 2020 #138}], and the overall human population graph has gradually risen over the past 50 years [{Di Maria, 2018 #174}]. As the population increases, food consumption rises proportionally. Consequently, food-related waste materials also increase daily [{Erdem, 2021 #136}]. A large amount of organic waste is produced globally each year [{Khan, 2023 #169}]. Approximately 1.3 billion tons of solid waste are collected worldwide [{Kaur, 2023 #175}]. This waste is often disposed of in the environment or landfills, where it decomposes into pollutants [{Srivastava, 2020 #176}]. By-products generated during harvesting or farming are typically classified as waste [{Westerman, 2005 #137}]. Biowaste refers to organic waste derived from biological materials [{Srivastava, 2023 #178}]. It is sustainable due to the renewable nature of its biochemical compounds [{Safian, 2020 #144}]. Biowaste includes various types, such as animal manure, crop residues, and food processing waste [{Fernández-López, 2004 #139}].

Biowastes are collected from diverse sources, including municipal waste, agricultural waste, and vegetable market waste [{Hasan, 2023 #179}]. They are classified into agricultural waste, industrial waste, municipal solid waste (MSW), and forest residues [{Rajkumar, 2022 #177}]. Several methods are used to utilize and process biowaste [{Devi, 2023 #180}] to convert waste into useful resources [{Sakhiya, 2020 #142}], especially agricultural residues, which are particularly suitable for pyrolysis and charcoal production [{Fernández-López, 2004 #168}; {Sait, 2012 #141}]. People affected by poverty are often unable to access or afford basic necessities [{Guan, 2023 #164}]. Additionally, the Earth's climate is impacted by the excessive use of energy resources in daily life and across various sectors [{Basumatary, 2023 #172}; {Reddy, 2019 #173}; {Holechek, 2022 #170}; {Monga, 2023 #171}]. One of the safest

and most effective alternatives is the production of charcoal from biowaste, which is more efficient, affordable, and less costly than fossil fuels [{Kanwal, 2022 #165}].

Charcoal is a viable method to utilize the energy contained in biowaste [{Meyer, 2011 #145}]. It is produced using waste materials [{Cha, 2016 #146}] and consists primarily of carbon, formed through pyrolysis [{Ganesh, 2022 #182}] into a black, graphite-like structure [{Ravichandran, 2018 #186}; {Aschemann-Witzel, 2015 #167}], with a lower combustion ability [{Peng, 2023 #166}]. It is widely used to remove a broad range of pollutants from water and wastewater [{Mohammad-Khah, 2009 #143}]. Charcoal made from biowaste contains several components, with carbon (C) being the main one [{Dıaz-Teran, 2001 #147}]. Its beneficial effects stem from its high porosity [{Hale, 2016 #183}], great mechanical strength, and significant adsorption capacity [{El-Shafey, 2010 #189}]. Activation enhances the porosity and surface area of the charcoal [{Neolaka, 2023 #185}]. Compared to traditional sources, charcoal from non-traditional sources such as biowaste is more economical [{Zabihi, 2010 #188}].

Natural materials mainly consist of carbon atoms [{Alaqarbeh, 2021 #149}]. Charcoal functions through the process of adsorption [{Lam, 2020 #148}], which is the accumulation of molecules on the surface of a solid due to physical or chemical bonding [{Yagub, 2014 #150}]. The substance that accumulates is known as the adsorbate, while the material that collects it is the adsorbent [{Shakoor, 2017 #151}; {Ören, 2006 #152}]. Adsorption can be classified into physical adsorption and chemical adsorption, depending on the nature of the intermolecular forces [{Ashtaputrey, 2020 #153}; {Ahmed, 2022 #162}]. It is widely used for the purification and removal of contaminants from air, soil, and beverages [{Mopoung, 2015 #156}; {Ajala, 2022 #155}]. Adsorption is used for the removal of dyes, suspended particles, and heavy metals [{Lupaşcu, 2020 #157}]. Granular activated carbon (GAC) is commonly used to adsorb harmful gases and toxic fumes [{Heidarinejad, 2020 #158}; {Décima, 2021 #159}], while powdered activated carbon (PAC), which is finely ground, is mainly employed in bleaching processes to remove dyes and heavy metals [{Xin, 2020 #160}; {Genli, 2022 #161}].

Various materials are used to prepare different types of carbon-based activated charcoal [{Luisetto, 2023 #163}], and the characteristics of charcoal vary depending on the preparation method [{Rahman, 2006 #154}]. Over recent years, industries have produced significant waste, including dyes and heavy metals, that are highly polluting to the environment [{Shamsuddin, 2016 #190}; {Crini, 2019 #184}; {Yahya, 2018 #187}]. The focus of this research is on the

production of charcoal from biowaste [{Duangkham, 2023 #181}], which is converted into ash at high temperatures through reactions with oxygen [{Prasun, 2023 #191}]. Carbon-based technologies are being explored for future sustainable resource management [{Pandey, 2023 #192}].

This study specifically explores the creation and analysis of charcoal derived from local waste materials, particularly banana and potato peels. These organic wastes, which are often discarded, have the potential to be converted into high-quality activated carbon. The goal is to develop a sustainable and environmentally friendly method for charcoal production using these readily available biowastes. The research investigates how banana and potato peels can be transformed into effective adsorbents—materials capable of trapping and removing impurities from liquids or gases. By doing so, the project promotes practical waste management solutions with significant environmental benefits. This approach may lead to innovative recycling strategies for agricultural residues, reduce waste, and provide a low-cost alternative to traditional activated carbon.

Experimental

Fresh peel samples of potato (*Solanum tuberosum*) and banana (*Musa acuminata*) were collected from local market. The samples were first washed with tap water at room temperature. For oven drying, the samples were placed in an oven at 100 °C for 8 hours; for sun drying, they were exposed to sunlight for two to three days. Subsequently, both types of samples were washed with distilled water and dried again in the oven at 100 °C for 6 hours. The dried samples were separately subjected to carbonization using a muffle furnace set at 500 °C for 30 minutes. The resulting charcoal was ground using a pestle and mortar to increase its surface area. Each sample was then sieved individually using a 140-mesh sieve for 10 minutes with a sieve shaker. Finally, the charcoal produced from banana and potato peels was combined in varying ratios ranging from 0 to 10.

Materials

Chemicals

Charcoal (2 g) of all ratios were placed in the HCl (15 ml, 0.5 N) and NaOH (15 ml, 0.5 N) solutions for 24 h filter by adding distilled water to neutralize the pH then the retentate was placed for 24 h to dry the remaining moisture.

Characterization

Moisture content and Ash content are engineering applications used for handling and storage. At the temperature of 100℃, using a sample (0.5 g) for 2 h. For ash content, place them in the muffle furnace for 6 h at 600℃ and then weigh them [{Standard, 2013 #193}, {Mujtaba, 2021 #194}].

Add iodine solution (5 ml) to charcoal (0.2 g). Centrifuge the mixture for 3 min. Titrate with the prepared standard sodium thiosulphate solution. The titration process continues until the iodine's bright yellow color turns pale yellow. Add 5 drops of starch solution until it becomes colorless [{Madu, 2013 #195}, {Yusufu, 2012 #196}]. Add prepared methylene blue solution drop by drop in of charcoal (0.1 g) and swirl until no more methylene blue solution adsorbed [{Thang, 2021 #197}].

PSA was used to identify the charcoal particle size. FTIR is widely used for identifying functional groups and the chemical composition of substances based on their molecular vibration [{Rafique, 2021 #198}, {Nandiyanto, 2019 #201}]. X-ray diffraction was carried out to examine the crystal structure of synthesized samples [{Kubra, 2022 #199}]. FE-SEM analysis morphological characteristics and elemental composition and were identified at the microscale and nanoscale [{Fatima, 2024 #200}].

Adsorption optimization

Adsorbent dose

Equilibrium isotherms were investigated by adding 71.4, 142.8, 214.3, 285.7, and 357.1 ppm of methylene blue dye to distilled water (100 ml). The pH level of the solution was adjusted to a neutral state. Each solution was agitated at a room temperature of 25 ± 1°C [{Kassahun, 2022 #202}]. Table 1 shows the values of different factors of the experimental conditions.

Initial concentration

Equilibrium isotherms were investigated by adding 0.05 g, 0.10 g, 0.15 g, 0.20 g, and 0.25 g of charcoal to methylene blue solutions (100 ml). The solution's pH level was adjusted to a neutral state. The quantity of charcoal that resulted in the highest removal of methylene blue was consistently used for every adsorption isotherm test. Each solution was agitated at a room temperature of 25 ± 1°C [{Kassahun, 2022 #202}]. Table 1 shows the values of different factors of the experimental conditions.

Contact time

Equilibrium isotherms were investigated by adding charcoal (0.1 g) to methylene blue solution (100 ml). The solution's pH level was adjusted to a neutral state. The solution of methylene blue was obtained after a specific interval, about 5 minutes. The solution was agitated at a room temperature of 25 ± 1°C [{Kassahun, 2022 #202}]. Table 1 shows the values of different factors of the experimental conditions.

Table 1 **Variable factors for Equilibrium isotherms**

Factor	Contact Time (min)	Adsorbent Dose (g)	Initial concentration (ppm)
1	5,10,15,20,25,30,35,40	0.10	100
2	30	0.05,0.10,0.15,0.20.0.25	100
3	30	0..10	71.4,142.8,214.3,285.7,357.1

Adsorption isotherms

The Langmuir isotherm posits that maximum adsorption occurs when a single layer of adsorbate entirely covers the surface of the adsorbent. The Freundlich isotherm posits that maximum adsorption occurs when a multi layer of adsorbate covers the surface of the adsorbent [{Kassahun, 2022 #202}].

Results and discussion

Optimization of Charcoal

Fresh potato and banana peel samples were collected. These peels were dried in different conditions after washing. After that washed with distilled water and dried in the oven. Dried samples were placed separately in the muffle furnace to form charcoal. That was grounded by using a pestle mortar and sieved. Sieved samples were combined in different ratios. Samples of all ratios were activated with HCl and NaOH.

Characterization of adsorbent

Proximate analysis

Charcoal with a low moisture content is preferred because it improves combustion and energy output, making the charcoal burn more efficiently. Properly kiln-dried charcoal usually contains 1-5% moisture {Mujtaba, 2021 #208}, {Madu, 2013 #209}.

A lower ash content is typically preferred, as higher ash content can reduce the efficiency of combustion and produce more waste. Charcoal usually has an ash content ranging from 1-3%. A higher iodine value indicates a greater surface area and higher adsorption capacity, making it more effective {Mujtaba, 2021 #208}, {Madu, 2013 #209}.

A higher iodine value signifies better adsorptive properties, ranging from 100 to 500 mg/g {Yusufu, 2012 #210}, {Thang, 2021 #211}].

The amount of methylene blue dye that can be adsorbed by a given mass of charcoal, reflects the material's surface area and porosity. Charcoal may have a significantly lower methylene blue value, often below 100 mg/g [{Standard, 2013 #207}. Table 2 shows the values of different factors of the experimental conditions.

Table 2 **Proximate analysis of various charcoal**

Parameters	Values					
	SNC	ONC	SAC	OAC	SBC	OBC
Moisture content	0.05%	0.028%	0.029%	0.062%	0.025%	0.134%
Ash content	1.36%	1.70%	0.22%	0.36%	0.20%	0.28%

Iodine value	492	452	460	460	495	460
Methylene blue value	45	52	51	66	90	81

Particle Size Analysis (PSA)

The PSA of the charcoal is used to identify the size of the charcoal produced for carrying out the reaction. It shows the size of the particles was about 1000 nm. The smaller the size of particles larger the surface area. The R^2 value, which reflects how closely the experimental data aligns, was determined to be 0.9842 by using the Gaussian fit model.

Fourier Transform Infrared Spectrophotometer

FTIR identified all functional groups before and after the activation with HCl and NaOH. Complex compounds were also identified by identifying various functional groups.

In the FTIR spectrum, various peaks are shown. These peaks are at 1379.12 for the C-H methylene group, 1580.39 for C=C-C aromatic ring stretching, 2117.13 for the terminal alkylene group of the chain, 2855.14, and 2922.23 for the C-H stretching vibration of methylene group which shows the different functional groups. 2855.14 and 2922.23 both show the stretching vibrations of the methylene group. All these functional groups are pure carbon in nature, these are mainly alky, alkylene, and aromatic groups. These groups show that the formed charcoal is only composed of pure carbon. While FTIR of the charcoal that adsorbed methylene blue shows the peaks of the carbon as well as the peak of the methylene blue at 1364.206 [{Rafique, 2021 #205}, {Nandiyanto, 2019 #206}]. Fig. 1 shows FTIR of Charcoal.

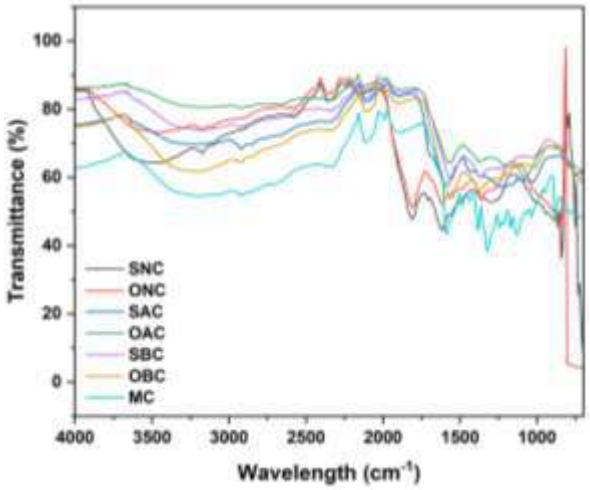

Fig. 1 FTIR of Charcoal

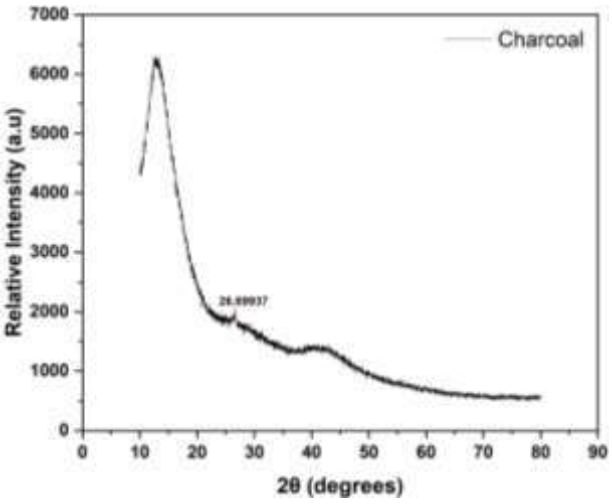

Fig. 2 XRD of Charcoal

X-Ray Diffraction

By studying the graph obtained through the XRD of the charcoal. The graph shows the highest and the single peak at the point of 26.356 Å, it is the only peak which is of the carbon compound. Hump-like structures were also observed which shows the compound was amorphous [{Kubra, 2022 #204}]. Fig. 2 shows XRD of Charcoal.

Scanning Electron Microscope (SEM)

Scanning electron microscopy (SEM) investigated powdered charcoal's surface morphology and microstructure, showing characteristics of surface texture, porosity, particle size and shape, and even microstructure details together with EDX analysis. SEM scans depict

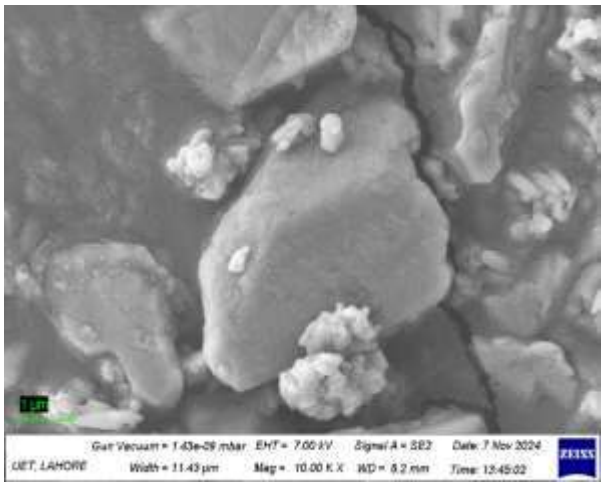

numerous pores contributing to charcoal's extensive surface area, enhancing its adsorption effectiveness.

The SEM analysis yields comprehensive information about the amorphous or fragmented appearance and the particle size and shape of the charcoal powder. Fig. 3 shows SEM of Charcoal.

Microstructural Details depend on the magnification, the SEM images may reveal fine cracks, voids, or particles indicating the disintegration of larger carbonaceous material. EDX shows charcoal was rich in carbon and oxygen compounds while lower concentrations of Na, Mg, Si, K, and Ca were observed [{Fatima, 2024 #203}]. Fig. 4 shows EDX of Charcoal.

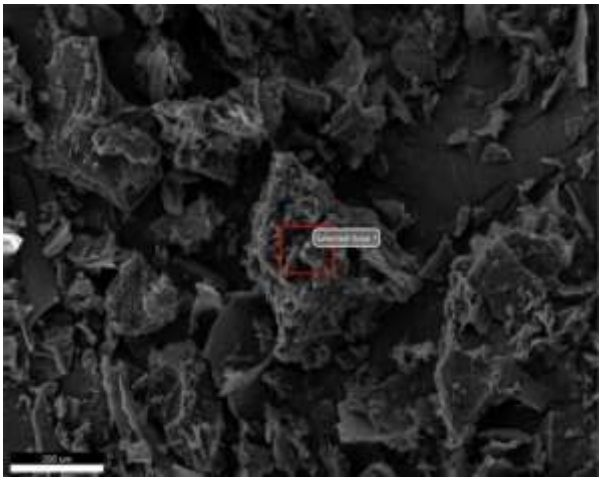

Fig. 3 SEM of Charcoal

Fig. 4 *EDX of Charcoal*

Adsorption optimization

Effect of Adsorbent dose

Methylene blue was optimized with the help of 0.1 g of charcoal for a specific time of about 30 minutes so that the highest amount of degradation occurs at 214 ppm of the concentration, which is about 69.4%. The R^2 value, which reflects how closely the experimental data aligns with the standard curve, was determined to be 0.9947. The linear plots' intercepts and slopes yield 1243.7 mg/g and 0.3132 L/g, respectively [{Kassahun, 2022 #202}]. Fig. 7 shows Degradation of Adsorbent Dose.

Initial concentration

Charcoal was optimized with 1500 ppm of Methylene blue for a specific time of about 30 minutes so that the highest degradation occurs at 0.25 g of the charcoal amount, which is about 37.3% [{Kassahun, 2022 #202}]. Fig. 5 shows Degradation of Initial Concentration.

Contact time

Methylene blue was optimized with the help of 0.1 g of charcoal for a specific time of about 30 minutes so that the highest amount of degradation occurs at 214 ppm of the concentration, which is about 69.4% [{Kassahun, 2022 #202}]. Fig. 6 shows Degradation of Contact Time.

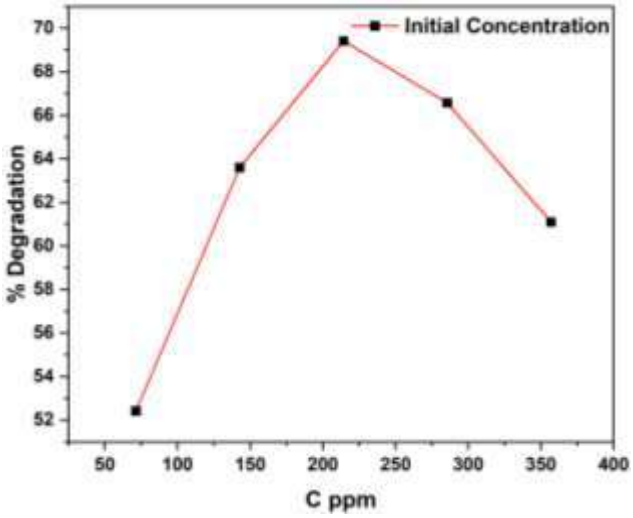

Fig. 5 Degradation of Initial Concentration

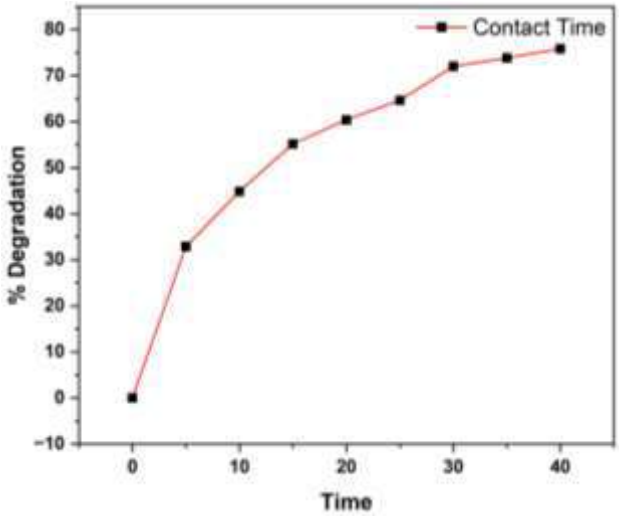

Fig. 6 Degradation of Contact Time

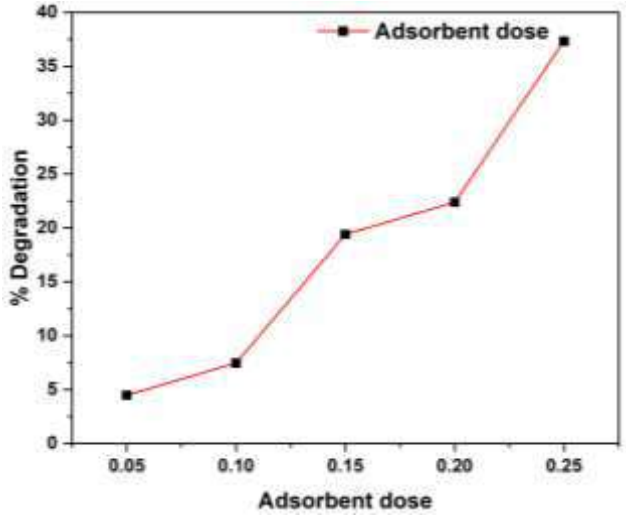

Fig. 7 Degradation of adsorbent dose

Adsorption isotherms

The R^2 value, which reflects how closely the experimental data aligns with the Langmuir isotherm model, was determined to be 0.99981. The parameters q_m and K_L for the adsorbent were calculated from the intercepts and slopes of the linear plots, yielding values of 3.2337 mg/g and -1.3303 L/g, respectively [{Kassahun, 2022 #202}]. Fig. 8 shows Langmuir Isotherm model.

The R^2 value, which reflects how closely the experimental data aligns with the Freundlich isotherm model, was determined to be 0.66456. The parameters $1/n$ and K_F for the adsorbent were calculated from the intercepts and slopes of the linear plots, yielding values of 10.93139 mg/g and 1.57419 L/g, respectively [{Kassahun, 2022 #202}]. Fig. 9 shows Freundlich Isotherm model and Table 3 shows a comparison between Langmuir and Freundlich isotherm models.

Table 3 **Comparison of Langmuir and Freundlich Isotherm Models**

Langmuir isotherm parameters				Freundlich isotherm parameters			
Equation	R^2	K_L (L/g)	q_m (mg/g)	Equation	R^2	K_F (L/g)	$1/n$
Y=a+b*x	0.99981	-1.3303	3.2337	Y=a+b*x	0.66456	1.57419	10.93139

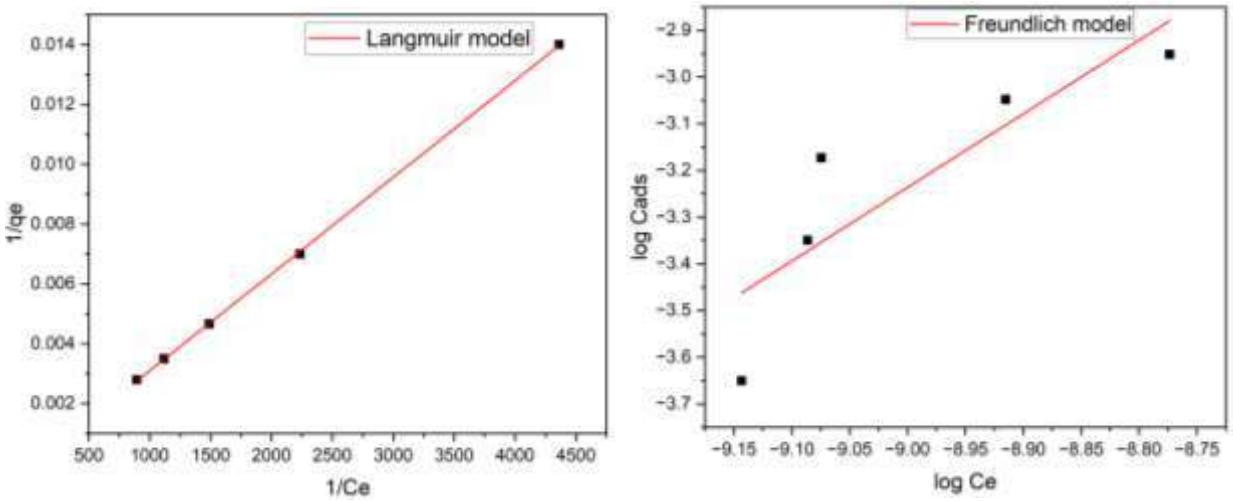

Fig. 8 Langmuir Isotherm model

Fig. 9 Freundlich Isotherm Model

Conclusions

In this study, biowaste from bananas and potatoes was used for the preparation of charcoal and to investigate its adsorption performance in a combined form. Charcoal was prepared by the pyrolysis of sun-dried and oven-dried biowaste at 500 °C separately, followed by sieving through a 140-mesh screen. The prepared charcoal from both biowastes was then combined in different ratios. The samples were prepared in their native form and activated under acidic conditions using HCl and under alkaline conditions using NaOH. Characterization of the native, acid-activated, and base-activated forms was performed using XRD, FTIR, SEM, EDX, methylene blue value, iodine value, ash content, and moisture content. Among the samples, the best results for SNC were observed at the P1:B9 ratio, for ONC at P10:B0, for SAC at P8:B2, for OAC at P0:B10, for SBC at P0:B10, and for OBC at P10:B0. These optimal ratios were determined based on moisture content, ash content, iodine value, and methylene blue value. Among all tested ratios, the best overall performance was exhibited by the SBC sample (P0:B10), due to its low moisture content, low ash content, and high iodine and methylene blue values. EDX analysis showed that the charcoal contained approximately 6% impurities. FTIR analysis revealed the presence of aromatic C-H bending and aromatic ring structures. The application of charcoal in methylene blue dye adsorption indicated that the optimal adsorbent dose was 0.25 g, with a contact time of 40 minutes and an initial dye concentration of 214 ppm. Equilibrium data were best described by the Langmuir isotherm model, with an R^2 value of 0.999, indicating a monolayer adsorption process. The results from characterization and application studies demonstrate that the prepared charcoal from banana and potato biowaste is effective and possesses a high adsorption capacity.

.

Symbols

Subscripts

SNC Sun-dried native charcoal

ONC oven-dried native charcoal

SAC Sun-dried acid activated charcoal

OAC oven-dried acid activated charcoal

SBC sun-dried base activated charcoal

OBC oven-dried base activated charcoal

Ethics Approval

All authors have read, understood, and complied as applicable with the statement. No permissions or licenses were necessary to collect the samples used in study.

Consent of participation

All authors made significant contributions to the manuscript and agree to its publications.

Consent of publication

Consent of publication given to the journal.

Data Availability

The data that helps identify the findings and results of the study are included in this paper.

Competing interests

The authors declare no known competing financial interests or personal relationships affecting the research or conclusions of the work published.

Funding

There is no funding provided for this research work.

Acknowledgements

We want to thank the University of Engineering and Technology for providing us with support and laboratory facilities.

References

1. Pradhan, S., et al., *Biochar from vegetable wastes: agro-environmental characterization.* Biochar, 2020. **2**: p. 439-453.
2. Rico, D., et al., *Extending and measuring the quality of fresh-cut fruit and vegetables: a review.* Trends in Food Science & Technology, 2007. **18**(7): p. 373-386.
3. Pokharel, P., Z. Ma, and S.X. Chang, *Biochar increases soil microbial biomass with changes in extra-and intracellular enzyme activities: a global meta-analysis.* Biochar, 2020. **2**: p. 65-79.
4. Erdem, H., *The effects of biochars produced in different pyrolsis temperatures from agricultural wastes on cadmium uptake of tobacco plant.* Saudi Journal of Biological Sciences, 2021. **28**(7): p. 3965-3971.
5. Westerman, P. and J. Bicudo, *Management considerations for organic waste use in agriculture.* Bioresource technology, 2005. **96**(2): p. 215-221.
6. Foong, S.Y., et al., *Valorization of biomass waste to engineered activated biochar by microwave pyrolysis: Progress, challenges, and future directions.* Chemical Engineering Journal, 2020. **389**: p. 124401.
7. Fernández-López, J., et al., *Application of functional citrus by-products to meat products.* Trends in Food Science & Technology, 2004. **15**(3-4): p. 176-185.
8. Aschemann-Witzel, J., et al., *Consumer-related food waste: Causes and potential for action.* Sustainability, 2015. **7**(6): p. 6457-6477.

9. Sait, H.H., et al., *Pyrolysis and combustion kinetics of date palm biomass using thermogravimetric analysis.* Bioresource Technology, 2012. **118**: p. 382-389.

10. Sakhiya, A.K., A. Anand, and P. Kaushal, *Production, activation, and applications of biochar in recent times.* Biochar, 2020. **2**: p. 253-285.

12. Mohammad-Khah, A. and R. Ansari, *Activated charcoal: preparation, characterization and applications: a review article.* Int J Chem Tech Res, 2009. **1**(4): p. 859-864.

13. Safian, M., H. Motaghian, and A. Hosseinpur, *Effects of sugarcane residue biochar and P fertilizer on P availability and its fractions in a calcareous clay loam soil.* Biochar, 2020. **2**: p. 357-367.

14. Meyer, S., B. Glaser, and P. Quicker, *Technical, economical, and climate-related aspects of biochar production technologies: a literature review.* Environmental science & technology, 2011. **45**(22): p. 9473-9483.

15. Cha, J.S., et al., *Production and utilization of biochar: A review.* Journal of Industrial and Engineering Chemistry, 2016. **40**: p. 1-15.

16. Dıaz-Teran, J., et al., *Porosity and adsorption properties of an activated charcoal.* Colloids and Surfaces A: Physicochemical and Engineering Aspects, 2001. **187**: p. 167-175.

17. Lam, S.S., et al., *Engineering pyrolysis biochar via single-step microwave steam activation for hazardous landfill leachate treatment.* Journal of hazardous materials, 2020. **390**: p. 121649.

18. Alaqarbeh, M., *Adsorption phenomena: definition, mechanisms, and adsorption types: short review.* RHAZES: Green and Applied Chemistry, 2021. **13**: p. 43-51.

19. Yagub, M.T., et al., *Dye and its removal from aqueous solution by adsorption: a review.* Advances in colloid and interface science, 2014. **209**: p. 172-184.

20. Shakoor, S. and A. Nasar, *Adsorptive treatment of hazardous methylene blue dye from artificially contaminated water using cucumis sativus peel waste as a low-cost adsorbent.* Groundwater for Sustainable Development, 2017. **5**: p. 152-159.

21. Ören, A.H. and A. Kaya, *Factors affecting adsorption characteristics of Zn2+ on two natural zeolites.* Journal of hazardous materials, 2006. **131**(1-3): p. 59-65.

22. Ashtaputrey, P. and S. Ashtaputrey, *Preparation and characterization of activated charcoal derived from wood apple fruit shell.* J. Sci. Res, 2020. **64**(01): p. 236-240.

23. Rahman, M., et al., *Preparation and characterization of activated charcoal as an adsorbent.* Journal of Surface Science and Technology, 2006. **22**(3/4): p. 133.

24. Ajala, L., et al., *Insights into purification of contaminated water with activated charcoal derived from hamburger seed coat.* International Journal of Environmental Science and Technology, 2022. **19**(7): p. 6541-6554.

25. Mopoung, S., et al., *Characterization and properties of activated carbon prepared from tamarind seeds by KOH activation for Fe (III) adsorption from aqueous solution.* The scientific world journal, 2015. **2015**(1): p. 415961.

27. Heidarinejad, Z., et al., *Methods for preparation and activation of activated carbon: a review.* Environmental Chemistry Letters, 2020. **18**: p. 393-415.

28. Décima, M.A., et al., *A review on the removal of carbamazepine from aqueous solution by using activated carbon and biochar.* Sustainability, 2021. **13**(21): p. 11760.

29. Xin, W., X. Li, and Y. Song, *Sludge-based mesoporous activated carbon: the effect of hydrothermal pretreatment on material preparation and adsorption of bisphenol A.* Journal of Chemical Technology & Biotechnology, 2020. **95**(6): p. 1666-1674.

30. Genli, N., et al., *Preparation and characterization of activated carbon from hydrochar by hydrothermal carbonization of chickpea stem: an application in methylene blue removal by RSM optimization.* International Journal of Phytoremediation, 2022. **24**(1): p. 88-100.

31. Ahmed, A.S., et al., *High surface area activated charcoal for water purification.* Journal of Composites Science, 2022. **6**(10): p. 311.

32. Luisetto, M., et al., *Activated Charcoal and Derivate Materials in Drugs and Biopharmaceutical Purification: Impurity Aspects.* J Mater Sci Nanotechnol, 2023. **11**(1): p. 105.

33. Guan, Y., et al., *Burden of the global energy price crisis on households.* Nature Energy, 2023. **8**(3): p. 304-316.

34. Kanwal, S., et al., *An integrated future approach for the energy security of Pakistan: Replacement of fossil fuels with syngas for better environment and socio-economic development.* Renewable and Sustainable Energy Reviews, 2022. **156**: p. 111978.

35. Peng, X., et al., *Recycling municipal, agricultural and industrial waste into energy, fertilizers, food and construction materials, and economic feasibility: a review.* Environmental Chemistry Letters, 2023. **21**(2): p. 765-801.

36. Khan, A.U., et al., *Utilization of biowaste for sustainable production of coal briquettes.* Energies, 2023. **16**(20): p. 7025.

37. Holechek, J.L., et al., *A global assessment: can renewable energy replace fossil fuels by 2050?* Sustainability, 2022. **14**(8): p. 4792.

38. Monga, D., et al., *Recent advances in various processes for clean and sustainable hydrogen production.* Nano-Structures & Nano-Objects, 2023. **33**: p. 100948.

39. Basumatary, B., et al., *Post-harvest waste to value-added materials: Musa champa plant as renewable and highly effective base catalyst for Jatropha curcas oil-based biodiesel production.* Bioresource Technology Reports, 2023. **21**: p. 101338.

40. Reddy, K.R., et al., *Polymeric graphitic carbon nitride (g-C3N4)-based semiconducting nanostructured materials: synthesis methods, properties and photocatalytic applications.* Journal of environmental management, 2019. **238**: p. 25-40.

41. Di Maria, F., F. Sisani, and S. Contini, *Are EU waste-to-energy technologies effective for exploiting the energy in bio-waste?* Applied Energy, 2018. **230**: p. 1557-1572.

42. Kaur, A., R. Bharti, and R. Sharma, *Municipal solid waste as a source of energy.* Materials Today: Proceedings, 2023. **81**: p. 904-915.

43. Srivastava, R.K., et al., *Sustainable energy from waste organic matters via efficient microbial processes.* science of the total environment, 2020. **722**: p. 137927.

44. Rajkumar, P. and S. Murugavelh, *Co-pyrolysis of wheat husk and residual tyre: Techno-economic analysis, performance and emission characteristics of pyro oil in a diesel engine.* Bioresource Technology Reports, 2022. **19**: p. 101164.

45. Srivastava, R.K., et al., *Valorization of biowastes for clean energy production, environmental depollution and soil fertility.* Journal of environmental management, 2023. **332**: p. 117410.

46. Hasan, M.R., et al., *Converting biowaste into sustainable bioenergy through various processes.* Bioresource Technology Reports, 2023: p. 101542.

47. Devi, C. and M. Khwairakpam, *Weed biomass: Bioconversion through composting followed by vermicomposting to optimize time required.* Bioresource technology reports, 2023. **21**: p. 101326.

49. Duangkham, S. and P. Thuadaij, *Characterization of charcoal briquettes produced from blending rice straw and banana peel.* Heliyon, 2023. **9**(6).

50. Ganesh, K.S., A. Sridhar, and S. Vishali, *Utilization of fruit and vegetable waste to produce value-added products: Conventional utilization and emerging opportunities-A review.* Chemosphere, 2022. **287**: p. 132221.

51. Hale, S.E., et al., *A synthesis of parameters related to the binding of neutral organic compounds to charcoal.* Chemosphere, 2016. **144**: p. 65-74.

52. Crini, G. and E. Lichtfouse, *Advantages and disadvantages of techniques used for wastewater treatment.* Environmental chemistry letters, 2019. **17**: p. 145-155.

53. Neolaka, Y.A., et al., *Potential of activated carbon from various sources as a low-cost adsorbent to remove heavy metals and synthetic dyes.* Results in Chemistry, 2023. **5**: p. 100711.

54. Ravichandran, P., et al., *Optimizing the route for production of activated carbon from Casuarina equisetifolia fruit waste.* Royal Society open science, 2018. **5**(7): p. 171578.

55. Yahya, M.A., et al. *A brief review on activated carbon derived from agriculture by-product*. in *AIP conference proceedings*. 2018. AIP Publishing.

57. Zabihi, M., A.H. Asl, and A. Ahmadpour, *Studies on adsorption of mercury from aqueous solution on activated carbons prepared from walnut shell.* Journal of hazardous materials, 2010. **174**(1-3): p. 251-256.

57. El-Shafey, E., *Removal of Zn (II) and Hg (II) from aqueous solution on a carbonaceous sorbent chemically prepared from rice husk.* Journal of hazardous materials, 2010. **175**(1-3): p. 319-327.

58. Shamsuddin, M., N. Yusoff, and M. Sulaiman, *Synthesis and characterization of activated carbon produced from kenaf core fiber using H3PO4 activation.* Procedia Chemistry, 2016. **19**: p. 558-565.

59. Prasun, A., et al., *Removal of Phenol from Biomedical Waste via an Adsorption Process.* Engineering Proceedings, 2023. **37**(1): p. 30.

60. Pandey, S., R.K. Shukla, and A. Srivastava, *TREATING WASTEWATER THROUGH ADSORPTION PROCESS BY USING AGRICULTURAL WASTE: A REVIEW.* Plant Archives (09725210), 2023. **23**(2).

61. ASTM, A., *Standard practice for proximate analysis of coal and coke.* Annu B Stand, 2013. **5**.

62. Mujtaba, G., et al., *Physio-chemical characterization of biochar, compost and co-composted biochar derived from green waste.* Sustainability, 2021. **13**(9): p. 4628.

63. Madu, P. and L. Lajide, *Physicochemical characteristics of activated charcoal derived from melon seed husk.* Journal of Chemical and Pharmaceutical Research, 2013. **5**(5): p. 94-98.

64. Yusufu, M., C. Ariahu, and B. Igbabul, *Production and characterization of activated carbon from selected local raw materials.* African journal of pure and applied chemistry, 2012. **6**(9): p. 123-131.

65. Thang, N.H., et al., *Methylene blue adsorption mechanism of activated carbon synthesised from cashew nut shells.* RSC advances, 2021. **11**(43): p. 26563-26570.

66. Rafique, S., I. Rashid, and R. Sharif, *Cost effective dye sensitized solar cell based on novel Cu polypyrrole multiwall carbon nanotubes nanocomposites counter electrode.* Scientific reports, 2021. **11**(1): p. 14830.

67. Kubra, K.T., et al., *Electrochemical investigation of a novel quaternary composite based on dichalcogenides, reduced graphene oxide, and polyaniline as a high-performance electrode for hybrid supercapacitor applications.* Journal of Alloys and Compounds, 2022. **909**: p. 164854.

68. Fatima, S., et al., *A novel binary composite of CuCoNi-MOF/MoO3 with exceptional capacitance as electrode material for supercapacitors.* Journal of Energy Storage, 2024. **99**: p. 113300.

69. Kassahun, E., et al., *The application of the activated carbon from cordia africana leaves for adsorption of chromium (III) from an aqueous solution.* Journal of Chemistry, 2022. **2022**(1): p. 4874502.

70. Nandiyanto, A.B.D., R. Oktiani, and R. Ragadhita, *How to read and interpret FTIR spectroscope of organic material.* Indonesian Journal of Science and Technology, 2019. **4**(1): p. 97-118.